



Article

Solvent Dependent Disorder in $M_2(\text{BzOip})_2(\text{H}_2\text{O})\cdot\text{Solvate}$ ($M = \text{Co}$ or Zn)

Laura J. McCormick ^{1,2,*} , Samuel A. Morris ^{2,3}, Simon J. Teat ¹, Alexandra M.Z. Slawin ² 
and Russell E. Morris ²¹ Advanced Light Source, Lawrence Berkeley National Laboratory, Berkeley, CA 94720, USA; sjteat@lbl.gov² School of Chemistry, University of St Andrews, North Haugh, St Andrews, Fife KY16 9ST, UK; smorris@ntu.edu.sg (S.A.M.); amzs@st-andrews.ac.uk (A.M.Z.S.); rem1@st-andrews.ac.uk (R.E.M.)³ Facility for Analysis, Characterisation, Testing and Simulation, Nanyang Technological University, Singapore 639798, Singapore

* Correspondence: ljmccormick@lbl.gov; Tel.: +1-510-495-2887

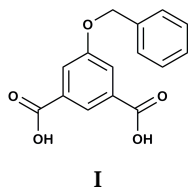
Received: 5 December 2017; Accepted: 19 December 2017; Published: 24 December 2017

Abstract: Coordination polymers derived from 5-benzyloxy isophthalic acid (H_2BzOip) are rare, with only three reported that do not contain additional bridging ligands, of which two $M_2(\text{BzOip})_2(\text{H}_2\text{O})$ ($M = \text{Co}$ and Zn) are isomorphous. It was hoped that by varying the solvent system in a reaction between H_2BzOip and $M(\text{OAc})_2$ ($M = \text{Co}$ and Zn), from water to a water/alcohol mixture, coordination polymers of different topology could be formed. Instead, two polymorphs of the existing $M_2(\text{BzOip})_2(\text{H}_2\text{O})$ ($M = \text{Co}$ and Zn) were isolated from aqueous methanol and aqueous ethanol, in which a small number of guest solvent molecules are present in the crystals. These guest water molecules disrupt the hexaphenyl embrace motif, leading to varying degrees of disorder of the benzyl groups.

Keywords: X-ray crystallography; solvothermal; polymorph; disorder

1. Introduction

Coordination polymers containing 5-substituted isophthalates have been, until recently, comparatively rare when compared to those containing the closely related terephthalate [1–15] and trimesate [16–18]. This family of ligands are of interest as they contain two carboxylate coordinating groups in a fixed geometry, while the 5-substituent is remote from these binding groups so that it can act as a structure-directing group without imposing a steric influence on the binding mode of the ligand. We recently reported a series of coordination polymers [19] derived from 5-alkoxy isophthalate ligands, in which the topology of the coordination polymers depended on which short chain alkyl group (ethyl, *n*-propyl, *n*-butyl or *i*-butyl) was present and what solvent was used. Given this solvent dependence of the topology of the coordination frameworks, it was hoped that the same would hold true when an aromatic substituent was used. The 5-benzyloxy isophthalic acid (H_2BzOip , **I**) was selected due to its similarity to the aforementioned 5-alkoxy isophthalic acids. It has been used as a bridging ligand in 11 coordination complexes to date [20–26], although all but three of these [26–28] include additional bridging or terminal polydentate ligands. Two of these, $M_2(\text{BzOip})_2(\text{H}_2\text{O})$ ($M = \text{Co}$ [26] or Zn [27]) have the same topology as the $M_2(\text{ROip})_2(\text{H}_2\text{O})$ ($M = \text{Mn}$, Co or Zn , $R = \text{Et}$, *n*Pr, *n*Bu or *i*Bu) materials reported in 2016, and were both prepared by hydrothermal reaction of H_2BzOip and the corresponding metal nitrate. By varying the solvent system from water to aqueous methanol, ethanol or *isopropanol*, it was found that, although the topology of the resulting $M_2(\text{BzOip})_2(\text{H}_2\text{O})$ ($M = \text{Co}$ or Zn) crystals did not vary, the level of disorder of the benzyl groups did. Herein, we report the crystal structures of the isostructural compounds $M_2(\text{BzOip})_2(\text{H}_2\text{O})\cdot\text{solvate}$ ($M = \text{Co}$ or Zn) as prepared from aqueous methanol, ethanol and *isopropanol*.



2. Results

All compounds were prepared by the solvothermal reaction of H_2BzOip and $\text{M}(\text{OAc})_2$ ($\text{M} = \text{Co}$ or Zn) in a 1:2 mixture of water and alcohol (methanol, ethanol, or *isopropanol*) and formed as purple or colourless needle crystals, respectively. $\text{M}_2(\text{BzOip})_2(\text{H}_2\text{O})\cdot\text{solvate}$ ($\text{M} = \text{Co}$ or Zn) crystallises in the trigonal space group $R\bar{3}$ with approximate unit cell dimensions $a \approx 28 \text{ \AA}$ and $c \approx 19 \text{ \AA}$. Details of the first crystal structure determination for each compound are presented in Table 1, whilst selected bond lengths and angles for all 18 structural determinations are given in Tables S1 to S36 in the Supporting Materials. The structure determinations of $\text{Zn}_2(\text{BzOip})_2(\text{H}_2\text{O})$ from *isopropanol* and ethanol are identical to that reported in [27], whilst the structure determination of $\text{Co}_2(\text{BzOip})_2(\text{H}_2\text{O})$ from *isopropanol* is identical to that reported in [26].

Two crystallographically distinct metal centres and two crystallographically distinct 5-benzyloxy isophthalate ligands are present in the asymmetric unit. One metal centre, M1, adopts a tetrahedral coordination environment in which one oxygen atom from each of the four unique carboxylate groups binds to the metal centre. Each of these carboxylate groups bind in an $(\eta^1:\eta^2:\mu_2)$ fashion, three of which connect M1 and M2 into a discrete unit that is reminiscent of a copper acetate lantern, whilst the fourth connects M1 to an M2 centre in an adjacent lantern-like unit. M2 adopts a square pyramidal geometry comprised of four carboxylate oxygen atoms (each from a distinct carboxylate group), and one water molecule. Both metal centres are also involved in long interactions (see Figure 1) with carboxylate oxygen atoms that are bound to the opposite metal centre that are deemed too long to be a coordination bond (approximate separations $\text{M1}\cdots\text{O}$ 2.9 and 2.9 \AA , and $\text{M2}\cdots\text{O}$ 3.1 and 3.3 \AA for Co and Zn, respectively).

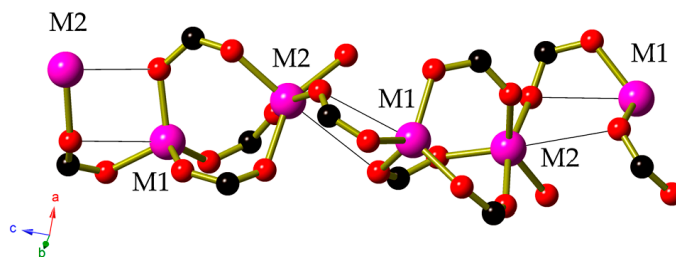


Figure 1. The coordination environment of the metal centres in $\text{Co}_2(\text{BzOip})_2(\text{H}_2\text{O})$. Long interactions between Co centres and carboxylate oxygen atoms are shown as thin black lines.

The isophthalate moiety of the 5-benzyloxy isophthalate ligand connects the metal centres into a honeycomb framework that may be seen in Figure 2. The panels that constitute the walls of the framework comprise pairs of isophthalate moieties, which are arranged parallel to each other with a plane-to-plane separation of approximately 3.6–3.7 \AA . Panels are connected to each other by infinite columns of metal centres and carboxylate groups that extend parallel to the c -axis, leaving large hexagonal channels parallel to the c -axis. The coordinated water molecules form hydrogen bonds to the coordinated carboxylate oxygen atoms and the phenolate oxygen atoms. The benzyloxy groups of the 5-benzyloxy isophthalate ligands project into and completely block these channels, where they form aggregates of six aromatic rings.

Table 1. Crystallographic data for the first run of the various $M_2(\text{BzOip})_2(\text{H}_2\text{O})$ crystals.

	Zn from MeOH	Zn from EtOH	Zn from <i>i</i> PrOH	Co from MeOH	Co from EtOH	Co from <i>i</i> PrOH
Molecular Formula	$\text{C}_{30.22}\text{H}_{23.35}\text{O}_{11.45}\text{Zn}_2$	$\text{C}_{30}\text{H}_{22}\text{O}_{11}\text{Zn}_2$	$\text{C}_{30}\text{H}_{22}\text{O}_{11}\text{Zn}_2$	$\text{C}_{30.29}\text{H}_{23.50}\text{Co}_2\text{O}_{11.58}$	$\text{C}_{30}\text{H}_{22.39}\text{Co}_2\text{O}_{11.19}$	$\text{C}_{30}\text{H}_{22}\text{Co}_2\text{O}_{11}$
Temperature	100(2)	173(2)	173(2)	100(2)	100(2)	173(2)
λ (Å)	0.7749	0.71075	0.71075	0.7749	0.7749	0.71075
Crystal System	Trigonal	Trigonal	Trigonal	Trigonal	Trigonal	Trigonal
Space Group	R3	R3	R3	R3	R3	R3
<i>a</i> (Å)	27.827(4)	27.759(3)	27.6973(18)	28.013(3)	27.877(3)	27.797(4)
<i>c</i> (Å)	18.255(2)	18.401(3)	18.2593(18)	18.1437(19)	18.192(2)	18.224(4)
<i>V</i> (Å ³)	12242(4)	12279(3)	12131(2)	12330(3)	12244(3)	12195(4)
<i>Z</i>	18	18	18	18	18	18
ρ (g cm ⁻³)	1.710	1.678	1.698	1.674	1.660	1.658
μ (mm ⁻¹)	2.309	1.822	1.844	1.609	1.617	1.282
<i>F</i> (000)	6413	6300	6300	6334	6227	6192
<i>Goof</i>	1.037	1.059	0.839	1.070	1.056	1.044
Reflections collected/unique/parameters	29,545/8105/467	42,033/6177/394	41,948/6193/394	29,077/8331/471	29,770/8248/441	41,642/6174/396
<i>R</i> _{int}	0.0712	0.0929	0.0862	0.0595	0.0565	0.1225
Final <i>R</i> indices (<i>I</i> > 2σ(<i>I</i>))	<i>R</i> 1 = 0.0506 <i>wR</i> 2 = 0.1476	<i>R</i> 1 = 0.0385 <i>wR</i> 2 = 0.0708	<i>R</i> 1 = 0.0349 <i>wR</i> 2 = 0.0575	<i>R</i> 1 = 0.0462 <i>wR</i> 2 = 0.1373	<i>R</i> 1 = 0.0405 <i>wR</i> 2 = 0.1109	<i>R</i> 1 = 0.0496 <i>wR</i> 2 = 0.0960
Final <i>R</i> indices (all data)	<i>R</i> 1 = 0.0593 <i>wR</i> 2 = 0.1550	<i>R</i> 1 = 0.0732 <i>wR</i> 2 = 0.0827	<i>R</i> 1 = 0.0616 <i>wR</i> 2 = 0.0629	<i>R</i> 1 = 0.0506 <i>wR</i> 2 = 0.1416	<i>R</i> 1 = 0.0471 <i>wR</i> 2 = 0.1156	<i>R</i> 1 = 0.1030 <i>wR</i> 2 = 0.1167

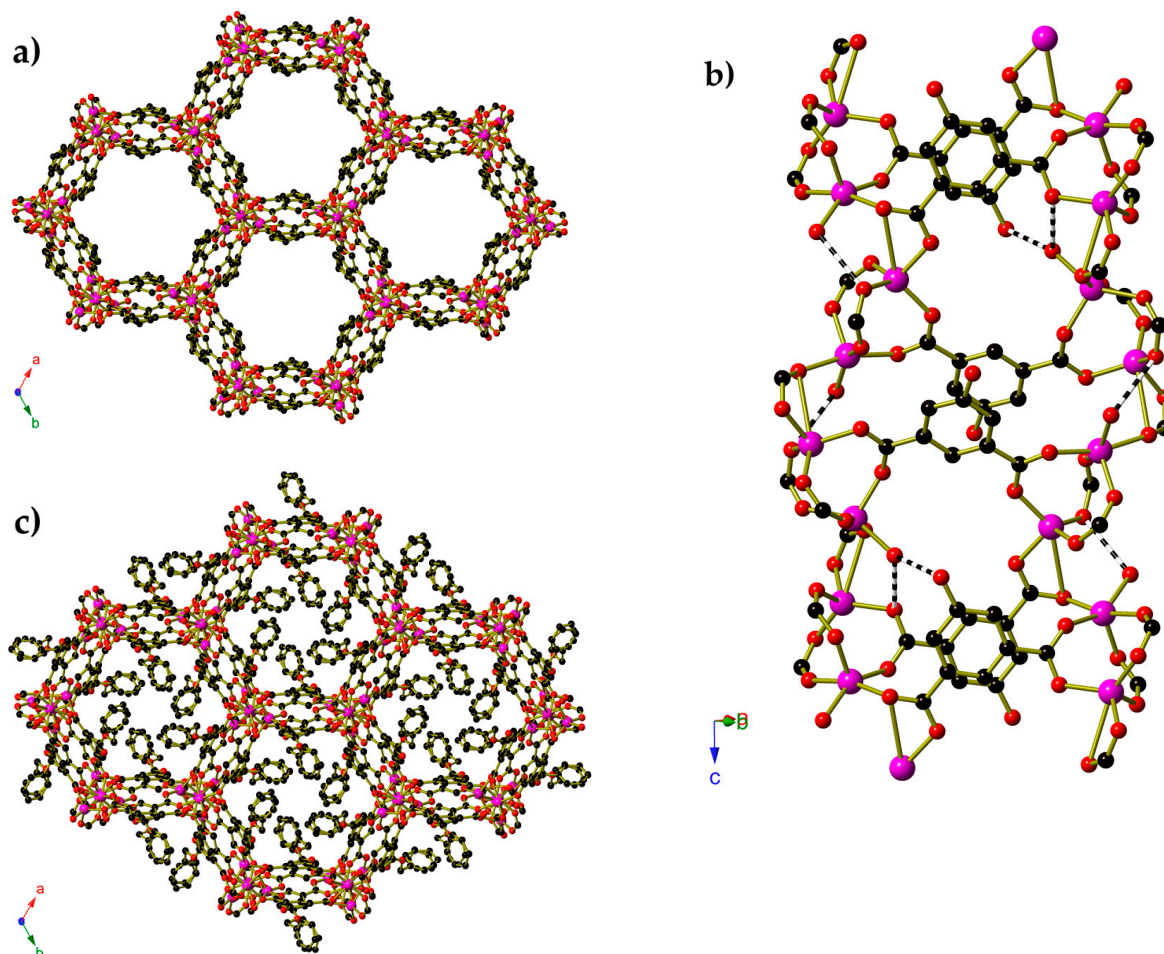


Figure 2. (a) A view along the *c*-axis of the honeycomb frameworks of $\text{Co}_2(\text{BzOip})_2(\text{H}_2\text{O})$ in which the benzyloxy groups have been removed for clarity; (b) one segment of the framework wall panels in $\text{Co}_2(\text{BzOip})_2(\text{H}_2\text{O})$, with the benzyl groups removed for clarity; and (c) a view of the full framework of $\text{Co}_2(\text{BzOip})_2(\text{H}_2\text{O})$.

As there are two crystallographically distinct ligands, two distinct hexaphenyl aggregates are formed (Figure 3). The first is well ordered in all six compounds and the six aromatic rings are involved in a hexaphenyl embrace [29]. Within this aggregate (shown using black carbon atoms and gold bonds in Figure 3), the methylene bridges connecting the benzyl group to the oxo isophthalate core are arranged around the equator of the aggregate. The arrangement of benzyl groups in the second aggregate varies from compound to compound. In both the $\text{Co}_2(\text{BzOip})_2(\text{H}_2\text{O})$ crystals from *i*PrOH, and the $\text{Zn}_2(\text{BzOip})_2(\text{H}_2\text{O})$ crystal from EtOH and *i*PrOH, these benzyl groups are well ordered and participate in a hexaphenyl embrace similar to that seen in the first aggregate, except that the methylene groups are located at the ‘poles’ of the aggregate. This aggregate is shown in Figure 3a using hatched black carbon atoms. In both the Zn and Co crystals from MeOH and the Co crystal from EtOH, this benzyl group is disordered over multiple orientations to accommodate the presence of partial occupancy solvent molecules. These solvent molecules participate in hydrogen bonding interactions with the carboxylate oxygen atoms and, in some instances, the coordinated water molecules.

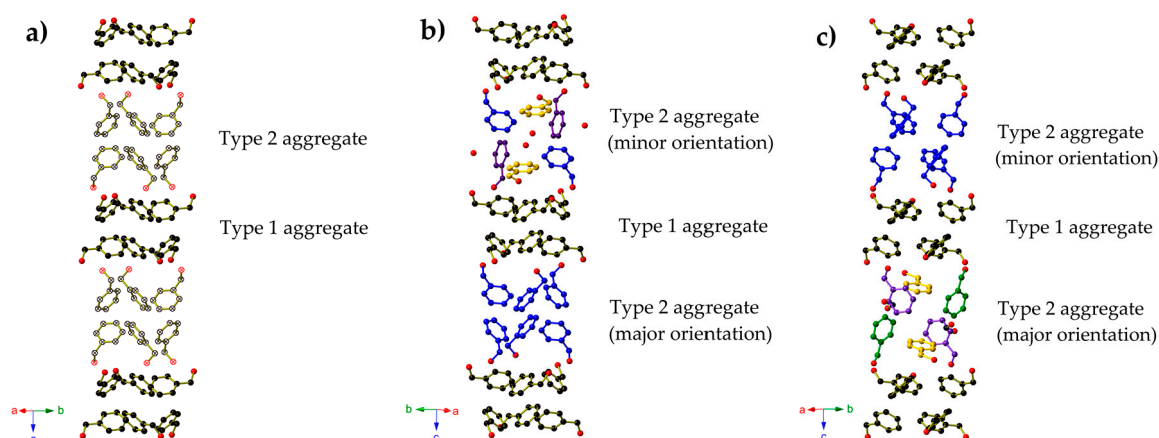


Figure 3. Views of the interactions between benzyl groups that occur in (a) $\text{Co}_2(\text{BzOip})_2(\text{H}_2\text{O})$ prepared in aqueous *isopropanol*; (b) $\text{Co}_2(\text{BzOip})_2(\text{H}_2\text{O})\cdot 0.19\text{H}_2\text{O}$ prepared in aqueous *ethanol*; (c) $\text{Co}_2(\text{BzOip})_2(\text{H}_2\text{O})\cdot 0.29\text{H}_2\text{O}\cdot 0.29\text{MeOH}$ prepared in aqueous *methanol*. In all cases, the benzyl groups shown in black are well ordered and participate in a hexaphenyl embrace. In (b) and (c), the benzyl groups shown in blue also participate in a hexaphenyl embrace. The hexaphenyl aggregate shown using hatched atoms in (a) is fully ordered in the crystals obtained from *isopropanol*, but disordered in the crystals obtained from *methanol* or *ethanol*.

In the $\text{Co}_2(\text{BzOip})_2(\text{H}_2\text{O})\cdot 0.19\text{H}_2\text{O}$ crystals from aqueous *ethanol*, the second aggregate of benzyl groups contains one major (shown in blue in Figure 3b) and three minor orientations. The three minor orientations are related by three-fold rotation in the *ab*-plane, and contain two benzyl groups from the major (blue) orientation, and two of each of the minor orientations of the benzyl group (shown in purple and yellow in Figure 3b). Whilst the major orientation of this aggregate results in a hexaphenyl embrace between the benzyl groups, the minor orientations contain a tetraphenyl embrace [30] between the benzyl groups coloured blue and purple in Figure 3b. Partial occupancy water molecules located near to this aggregate and the major orientation of the benzyl groups are positioned such that they are mutually exclusive, and the presence of the water molecules disrupts the hexaphenyl embrace of the major orientation. The ratio of the major to minor orientations of this aggregate are approximately 80:20. A close-up view of the minor orientation is shown in Figure 4a.

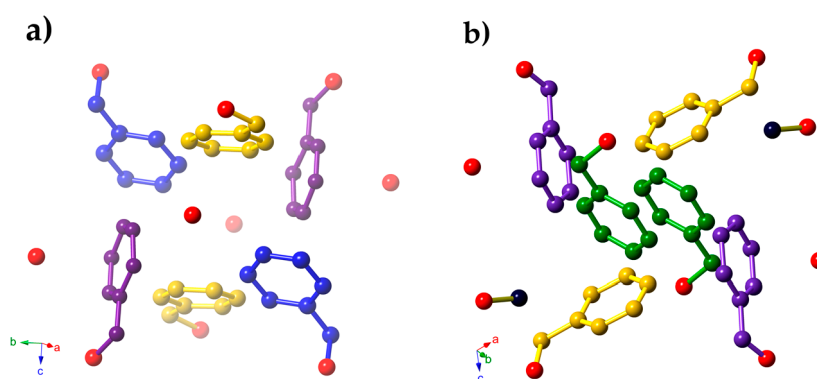


Figure 4. Views of the interactions between benzyl groups that occur in the disordered hexaphenyl aggregates in (a) $\text{Co}_2(\text{BzOip})_2(\text{H}_2\text{O})\cdot 0.19\text{H}_2\text{O}$ prepared in aqueous *ethanol*; and (b) $\text{Co}_2(\text{BzOip})_2(\text{H}_2\text{O})\cdot 0.29\text{H}_2\text{O}\cdot 0.29\text{MeOH}$ prepared in aqueous *methanol*. Benzyl groups depicted using the same colours are related by symmetry. Hydrogen atoms have been omitted for clarity.

In the $\text{M}_2(\text{BzOip})_2(\text{H}_2\text{O})\cdot 0.29\text{H}_2\text{O}\cdot 0.29\text{MeOH}$ ($\text{M} = \text{Co}$ or Zn) crystals, the second aggregate has three ‘major’ orientations and one minor orientation, and the two have no benzyl groups in common.

The minor orientation is comprised of six symmetry-related benzyl groups arranged into a hexaphenyl embrace (shown in blue in Figure 3c) in a very similar fashion to the major orientation of the second aggregate in $\text{Co}_2(\text{BzOip})_2(\text{H}_2\text{O})\cdot 0.19\text{H}_2\text{O}$. Conversely, the major orientations of this second orientation are similar to the minor orientation in $\text{Co}_2(\text{BzOip})_2(\text{H}_2\text{O})\cdot 0.19\text{H}_2\text{O}$, as the three major orientations are related by three-fold symmetry and are comprised of two of each of three further distinct benzyl group sites (shown in purple, green, and yellow in Figures 3c and 4b). The benzyl groups coloured yellow and green in Figure 3c participate in a tetraphenyl embrace. As with $\text{Co}_2(\text{BzOip})_2(\text{H}_2\text{O})\cdot 0.19\text{H}_2\text{O}$, there are solvent molecules present in the area surrounding the second benzyl aggregate that interferes with the hexaphenyl embrace motif. In these instances, there is a disordered water/methanol molecule that is mutually exclusive of the minor orientation of the aggregate and the green site of the major orientations (Figure 4b). In addition to this, the carbon atom of the methanol molecule lies too close to the purple benzyl ring site, resulting in two water molecules and two methanol molecules surrounding each of the major orientation aggregates. The ratio of the major to minor orientations is approximately 88:12 in the Co derivative, but 68:32 in the Zn derivative.

3. Discussion

In order to confirm that the disorder was not an aberration that occurred only in one crystal, single-crystal diffraction data was collected on three different crystals from the first batch of each of $\text{Co}_2(\text{BzOip})_2(\text{H}_2\text{O})\cdot 0.29\text{H}_2\text{O}\cdot 0.29\text{MeOH}$, $\text{Co}_2(\text{BzOip})_2(\text{H}_2\text{O})\cdot 0.19\text{H}_2\text{O}$, and $\text{Co}_2(\text{BzOip})_2(\text{H}_2\text{O})$, and two different crystals from a second batch of each. In all cases, the level of disorder was reasonably consistent between different crystals and different batches produced using the same synthetic conditions. In $\text{Co}_2(\text{BzOip})_2(\text{H}_2\text{O})\cdot 0.29\text{H}_2\text{O}\cdot 0.29\text{MeOH}$, the occupancy of the minor orientation of the disordered benzyl group (i.e., the one that forms hexaphenyl embraces, shown in blue in Figure 3c) varies from 9.6% to 12.6% in batch 1 and 12.1% to 15.9% in batch 2 (this occupancy was 32.3% in $\text{Zn}_2(\text{BzOip})_2(\text{H}_2\text{O})\cdot 0.23\text{H}_2\text{O}\cdot 0.22\text{MeOH}$). In $\text{Co}_2(\text{BzOip})_2(\text{H}_2\text{O})\cdot 0.19\text{H}_2\text{O}$, the occupancy of the major orientation of the disordered benzyl group (i.e., the one that forms hexaphenyl embraces, shown in blue in Figure 3b) varies from 78.4% to 81.0% in batch 1 and 77.9% to 79.9% in batch 2. Repeat structure determinations were not performed on $\text{Zn}_2(\text{BzOip})_2(\text{H}_2\text{O})\cdot 0.23\text{H}_2\text{O}\cdot 0.33\text{MeOH}$. Comparison of the calculated and experimental powder diffraction patterns for each of the 6 compounds is presented in Supporting Materials Figures S1–S6.

The progressive exclusion of solvent from the crystals is reflected in the thermogravimetric analysis (TGA) traces of the $\text{Co}_2(\text{BzOip})_2(\text{H}_2\text{O})\cdot \text{solvate}$ series (see Supporting Materials Figures S7–S12), with the mass loss step dropping from 5.07% for the crystals obtained from MeOH, to 3.83% from EtOH, to 2.79% from $i\text{PrOH}$, the latter corresponding to the approximate loss of the coordinated water molecule (2.66%). The mass losses from the corresponding $\text{Zn}_2(\text{BzOip})_2(\text{H}_2\text{O})\cdot \text{solvate}$ series all lie between 3.47 to 4.01% (MeOH and $i\text{PrOH}$, respectively). This suggests that the guest methanol is readily lost from the Zn crystals under ambient conditions.

In all crystals where disorder of the benzyl groups are observed, there are solvent (water and/or methanol) molecules present in the region of the hexaphenyl embraces making it sterically difficult for the type 2 benzyl groups to adopt the hexaphenyl embrace motif. This is noteworthy, as this does not occur when water alone is used as the preparative solvent, despite water being present in far greater amounts. We attribute this to the relative polarities of the solvent mixtures—the most and least polar solvent mixtures (water and aqueous *isopropanol*, respectively) see complete separation of the hydrophobic benzyl groups from the hydrophilic carboxylate groups and coordinated water molecules within the crystals in a manner that is similar to micelle formation. In the intermediate polarity solvent mixtures, aqueous methanol and ethanol, the micelle-type separation of the hydrophilic and hydrophobic sections of the ligand is incomplete as the solvent molecules participate in hydrogen bonding interactions to the phenolic oxygen atom, disrupting the formation of half of the hexaphenyl embrace motifs.

A similar pattern regarding the micelle-type separation of the hydrophilic carboxylate groups and hydrophobic alkyl chains was observed in coordination polymers derived from 5-alkoxy isophthalates. The presence of short alkyl chains in both the solvent system (e.g., MeOH) and the 5-alkoxy substituent (e.g., EtOip²⁻) afforded frameworks in which both alkyl chains and coordinated solvent molecules project into the channels. Frameworks isostructural to $M_2(\text{BzOip})_2(\text{H}_2\text{O})$ ($M = \text{Co}$ or Zn) were obtained when large hydrophobic alkyl chains were present in the ligand (e.g., ⁿBuOip²⁻), the solvent system (e.g., neat or aqueous ⁱPrOH), or both. Like the branched *isobutyl* chains, the benzyl group used in this study is too bulky to form the $M_6(\text{ROip})_5(\text{OH})_2(\text{H}_2\text{O})_4 \cdot x\text{H}_2\text{O}$ framework in which the alkyl chains and coordinated solvent both project into the same channels. It is worth noting that a related framework of composition $\text{Zn}(\text{BzNHip})$ ($\text{BzNHip}^{2-} = 5\text{-benzylamino isophthalate}$), which also contains hexagonal channels in which the benzyl substituents participate in hexaphenyl embrace interactions, was prepared from water and does not display any disorder of the benzyl substituents [31,32].

4. Materials and Methods

All reagents were obtained from commercial sources and were used without further purification.

4.1. Dimethyl 5-Hydroxy Isophthalate

Prepared using the literature method [33]. 5-Hydroxy isophthalic acid (9.11 g, 0.050 mol) was heated to reflux in a solution of conc. sulfuric acid (2.8 mL) in methanol (150 mL) for 16 h. The solution was cooled to room temperature, neutralised with saturated NaHCO_3 , and the solvent removed under reduced pressure. The residue was triturated in water (150 mL), and the inhomogeneous mixture extracted with dichloromethane (4×500 mL). The organic layers were collected, dried over magnesium sulfate, and the dichloromethane removed under reduced pressure. Yield: 9.21 g, 0.044 mol, 88%.

4.2. Dimethyl 5-Benzyloxy Isophthalate

Prepared using the literature method [34]. Dimethyl 5-hydroxy isophthalate (6.1 g, 0.029 mol) and freshly pulverised dry potassium carbonate (4.65 g, 0.034 mol) were suspended in a solution of acetone (50 mL) and acetonitrile (60 mL). The solution was allowed to reflux for approximately 1 h, and then benzyl chloride (3.65 g, 0.029 mol) was added dropwise. The mixture was allowed to reflux for a further 16 hours before cooling to room temperature and removing the solvent under reduced pressure. The residue was then completely taken up into a mixture of water (150 mL) and ethyl acetate (400 mL). The organic layer was isolated and washed with water (4×50 mL) until the aqueous layer reached pH 7. The organic layer was then washed with brine (50 mL), dried over sodium sulfate and the solvent removed under reduced pressure to afford a pale yellow oil that set into colourless crystals (9.75 g) upon cooling. The crystals were recrystallised from toluene/ethanol to give a pure product. Yield: 6.03 g, 0.020 mol, 70%.

4.3. 5-Benzyloxy Isophthalic Acid

Prepared using the literature method [34]. Dimethyl 5-benzyloxy isophthalate (3.95 g, 0.013 mol) was dissolved in a solution of potassium hydroxide (30.06 g, 0.54 mol) in methanol (300 mL) and the solution refluxed for approximately 2.5 h. The cooled solution was neutralised with 2M HCl. The white precipitate was collected by vacuum filtration, washed with water until the filtrate reached pH 7, and dried in a vacuum desiccator for 2 days. Yield: 3.13 g, 0.011 mol, 87%.

4.4. $M_2(\text{BzOip})_2(\text{H}_2\text{O}) \cdot \text{Solvate}$ ($M = \text{Co}$ or Zn)

Into a 23 mL Teflon-lined steel autoclave were placed 5-benzyloxy isophthalic acid (0.272 g, 1.00 mmol), and either $\text{Co}(\text{OAc})_2 \cdot 4\text{H}_2\text{O}$ (251 mg, 1.01 mmol) or $\text{Zn}(\text{OAc})_2 \cdot 2\text{H}_2\text{O}$ (0.220 g, 1.00 mmol), and the solids were suspended in a mixture of water (5 mL) and methanol (10 mL). The sealed autoclaves were placed into a 110 °C oven for 3 days. After this time, the autoclaves were cooled to

room temperature and the resulting purple (Co) or colourless (Zn) needle crystals were collected by vacuum filtration and washed with methanol. Yields:

$\text{Co}_2(\text{BzOip})_2(\text{H}_2\text{O}) \cdot 0.29\text{MeOH} \cdot 0.29\text{H}_2\text{O}$ from methanol: 280 mg, 0.41 mmol, 80%. Elemental analysis Calcd for $\text{C}_{30.29}\text{H}_{23.74}\text{O}_{11.58}\text{Co}_2$ C: 52.66 H: 3.46, Found C: 52.53 H: 3.31%.

$\text{Zn}_2(\text{BzOip})_2(\text{H}_2\text{O}) \cdot 0.22\text{MeOH} \cdot 0.23\text{H}_2\text{O}$ from methanol: 269 mg, 0.38 mmol, 77%. Elemental analysis Calcd for $\text{C}_{30.22}\text{H}_{23.34}\text{O}_{11.45}\text{Zn}_2$ C: 51.82 H: 3.36, Found C: 51.60 H: 2.86%.

$\text{Co}_2(\text{BzOip})_2(\text{H}_2\text{O}) \cdot 0.19\text{H}_2\text{O}$ from ethanol: Yields Co: 203 mg, 0.30 mmol, 59%. Elemental analysis Calcd for $\text{C}_{30}\text{H}_{22.38}\text{O}_{11.19}\text{Co}_2$ C: 53.01 H: 3.32, Found C: 52.80 H: 3.20%.

$\text{Zn}_2(\text{BzOip})_2(\text{H}_2\text{O})$ from ethanol: 266 mg, 0.39 mmol, 77%. Elemental analysis Calcd for $\text{C}_{30}\text{H}_{22}\text{O}_{11}\text{Zn}_2$ C: 52.28 H: 3.22, Found C: 52.15 H: 3.00%.

$\text{Co}_2(\text{BzOip})_2(\text{H}_2\text{O})$ from *isopropanol*: 246 mg, 0.36 mmol, 72%. Elemental analysis Calc for $\text{C}_{30}\text{H}_{22}\text{O}_{11}\text{Co}_2$ C: 53.27 H: 3.28, Found C: 53.01 3.35%.

$\text{Zn}_2(\text{BzOip})_2(\text{H}_2\text{O})$ from *isopropanol*: 320 mg, 0.46 mmol, 93%. Elemental analysis Calcd for $\text{C}_{30}\text{H}_{22}\text{O}_{11}\text{Zn}_2$ C: 52.28 H: 3.22, Found C: 52.28 H: 3.04%.

4.5. Crystallographic Analyses

All crystals were coated in a protective oil before being transferred to either a Bruker D8 diffractometer (Bruker, Madison, WI, USA) on station 11.3.1 at the Advanced Light Source ($\text{Co}_2(\text{BzOip})_2(\text{H}_2\text{O}) \cdot 0.29\text{MeOH} \cdot 0.29\text{H}_2\text{O}$ from methanol, $\text{Zn}_2(\text{BzOip})_2(\text{H}_2\text{O}) \cdot 0.22\text{MeOH} \cdot 0.23\text{H}_2\text{O}$ from methanol, and $\text{Co}_2(\text{BzOip})_2(\text{H}_2\text{O}) \cdot 0.19\text{H}_2\text{O}$ from ethanol, $\lambda = 0.77490 \text{ \AA}$) or a Rigaku Mercury2 SCXMiniflex (Rigaku, Tokyo, Japan) diffractometer ($\lambda = 0.71075 \text{ \AA}$) at the University of St. Andrews. Appropriate scattering factors were applied using XDISP [35] within the WinGX suite [36]. Multi-scan absorption corrections were applied to the synchrotron and in-house crystallographic data using SADABS [37] and REQAB [38] programs, respectively. Data were solved using SHELXT [39] or SHELXS-97 [40] and refined on F^2 using SHELXL-97 [41] using the ShelXle User interface [42]. All non-hydrogen framework atoms were refined with anisotropic thermal displacement parameters, with equivalent disordered atoms constrained to have equal U_{ij} values. All C-bound hydrogen atoms were included at their geometrically estimated position, while O-bound hydrogen atoms were located in the difference map and fixed at a distance of 0.90 \AA from the oxygen atom to which they are bound. Pairs of hydrogen atoms belonging to a single water molecule were also fixed at a distance of $1.47(2) \text{ \AA}$ from each other. Disorder of the benzyl groups was modelled initially from the difference map, with each orientation having a common occupancy such that the sum of all occupancies were constrained to sum to 1.00. Once all orientations were modelled, a visual inspection was conducted to determine which orientations were mutually exclusive within the hexaphenyl unit, and all occupancies were then defined relative to a single free variable. Atoms belonging to partial occupancy solvent molecules were initially modeled with an isotropic thermal displacement parameter fixed at 0.08 and their occupancy allowed to refine. Visual inspection was then conducted to see which orientations of the benzyl group were too close for this solvent molecule to be present, and the O (and C) atoms given an occupancy related to the existing single free variable.

5. Conclusions

The level of disorder of the pendant benzyl groups in the frameworks $\text{M}_2(\text{BzOip})_2(\text{H}_2\text{O}) \cdot \text{solvate}$ ($\text{M} = \text{Co}$ or Zn) was found to vary according to the polarity of the preparative solvent system used to produce the crystals, without changing the overall topology of the coordination framework. This demonstrates the more subtle ways that synthetic solvent choice can influence coordination polymer synthesis, even when the overall topology of the framework is not affected.

Supplementary Materials: The supplementary materials are available online at www.mdpi.com/2073-4352/8/1/6/s1. CCDC 1525893-1525897, 1526369-1526371, and 1526372-1526381 contain the supplementary crystallographic data for this paper. These data can be obtained free of charge from The Cambridge Crystallographic Data Centre via www.ccdc.cam.ac.uk/data_request/cif.

Acknowledgments: This work was funded by the British Heart Foundation (NH/11/8/29253) and the EPSRC (EP/K005499/1 and EP/K039210/1). This research used resources of the Advanced Light Source, which is a DOE Office of Science User Facility under contract no. DE-AC02-05CH11231.

Author Contributions: Laura J. McCormick conducted the synthetic work, crystallographic (in house) data collections and refinement, and prepared the manuscript. Samuel A. Morris performed the data collections at the ALS. Alexandra M. Z. Slawin, and Simon J. Teat secured funding for, and maintained the diffractometers at the University of St. Andrews and the Advanced Light Source, respectively. Russell E. Morris secured funding for the synthetic and operational aspects of this work and defined the initial project direction.

Conflicts of Interest: The authors declare no conflict of interest.

References

1. Cavka, J.H.; Jakobsen, S.; Olsbye, U.; Guillou, N.; Lamberti, C.; Bordiga, S.; Lillerud, K.P. A New Zirconium Inorganic Building Brick Forming Metal Organic Frameworks with Exceptional Stability. *J. Am. Chem. Soc.* **2008**, *130*, 13850–13851. [[CrossRef](#)] [[PubMed](#)]
2. Serre, C.; Millange, F.; Thouvenot, C.; Nogues, M.; Marsolier, G.; Louer, D.; Ferey, G. Very Large Breathing Effect in the First Nanoporous Chromium(III)-Based Solids: MIL-53 or $\text{Cr}^{\text{III}}(\text{OH})\cdot\{\text{O}_2\text{C}-\text{C}_6\text{H}_4-\text{CO}_2\}\cdot\{\text{HO}_2\text{C}-\text{C}_6\text{H}_4-\text{CO}_2\text{H}\}_x\cdot\text{H}_2\text{O}_y$. *J. Am. Chem. Soc.* **2002**, *124*, 13519–13526. [[CrossRef](#)] [[PubMed](#)]
3. Ferey, G.; Mellot-Draznieks, C.; Serre, C.; Millange, F.; Dutour, J.; Surble, S.; Margiolaki, I. A Chromium Terephthalate-Based Solid with Unusually Large Pore Volumes and Surface Area. *Science* **2005**, *309*, 2040–2042. [[CrossRef](#)] [[PubMed](#)]
4. Li, H.; Eddaoudi, M.; O’Keeffe, M.; Yaghi, O.M. Design and synthesis of an exceptionally stable and highly porous metal-organic framework. *Nature* **1999**, *402*, 276–279. [[CrossRef](#)]
5. Dietzel, P.D.C.; Blom, R.; Fjellvåg, H. Base-Induced Formation of Two Magnesium Metal-Organic Framework Compounds with a Bifunctional Tetratopic Ligand. *Eur. J. Inorg. Chem.* **2008**, *2008*, 3624–3632. [[CrossRef](#)]
6. Gao, Q.; Jiang, F.-L.; Wu, M.-Y.; Huang, Y.-G.; Wei, W.; Zhang, Q.-F.; Hong, M.-C. Crystal Structures, Topological Analyses, and Magnetic Properties of Manganese-Dihydroxyterephthalate Complexes. *Aust. J Chem.* **2010**, *63*, 286–292. [[CrossRef](#)]
7. Bloch, E.D.; Murray, L.J.; Queen, W.L.; Chavan, S.; Maximoff, S.N.; Bigi, J.P.; Krishna, R.; Peterson, V.K.; Grandjean, F.; Long, G.J.; et al. Selective Binding of O_2 over N_2 in a Redox-Active Metal–Organic Framework with Open Iron(II) Coordination Sites. *J. Am. Chem. Soc.* **2011**, *133*, 14814–14822. [[CrossRef](#)] [[PubMed](#)]
8. Dietzel, P.D.C.; Morita, Y.; Blom, R.; Fjellvåg, H. An In Situ High-Temperature Single-Crystal Investigation of a Dehydrated Metal–Organic Framework Compound and Field-Induced Magnetization of One-Dimensional Metal–Oxygen Chains. *Angew. Chem. Int. Ed.* **2005**, *44*, 6354–6358. [[CrossRef](#)] [[PubMed](#)]
9. Dietzel, P.D.C.; Panella, B.; Hirscher, M.; Blom, R.; Fjellvåg, H. Hydrogen adsorption in a nickel based coordination polymer with open metal sites in the cylindrical cavities of the desolvated framework. *Chem. Commun.* **2006**, 959–961. [[CrossRef](#)] [[PubMed](#)]
10. Sanz, R.; Martínez, F.; Orcajo, G.; Wojtas, L.; Briones, D. Synthesis of a honeycomb-like Cu-based metal–organic framework and its carbon dioxide adsorption behavior. *Dalton Trans.* **2013**, *42*, 2392–2398. [[CrossRef](#)] [[PubMed](#)]
11. Rosi, N.L.; Kim, J.; Eddaoudi, M.; Chen, B.; O’Keeffe, M.; Yaghi, O.M. Rod Packings and Metal–Organic Frameworks Constructed from Rod-Shaped Secondary Building Units. *J. Am. Chem. Soc.* **2005**, *127*, 1504–1518. [[CrossRef](#)] [[PubMed](#)]
12. Eddaoudi, M.; Kim, J.; Rosi, N.; Vodak, D.; Wachter, J.; O’Keeffe, M.; Yaghi, O.M. Systematic Design of Pore Size and Functionality in Isoreticular MOFs and Their Application in Methane Storage. *Science* **2002**, *295*, 469–472. [[CrossRef](#)] [[PubMed](#)]
13. Silva, C.G.; Luz, I.; Llabres i Xamena, F.X.; Corma, A.; Garcia, H. Water Stable Zr–Benzenedicarboxylate Metal–Organic Frameworks as Photocatalysts for Hydrogen Generation. *Chem. Eur. J.* **2010**, *16*, 11133–11138. [[CrossRef](#)] [[PubMed](#)]
14. Ahnfeldt, T.; Gunzelmann, D.; Loiseau, T.; Hirsemann, D.; Senker, J.; Ferey, G.; Stock, N. Synthesis and Modification of a Functionalized 3D Open-Framework Structure with MIL-53 Topology. *Inorg. Chem.* **2009**, *48*, 3057–3064. [[CrossRef](#)] [[PubMed](#)]

15. Biswas, S.; Couck, S.; Grzywa, M.; Denayer, J.F.M.; Volkmer, D.; Van Der Voort, P. Vanadium Analogues of Nonfunctionalized and Amino-Functionalized MOFs with MIL-101 Topology—Synthesis, Characterization, and Gas Sorption Properties. *Eur. J. Inorg. Chem.* **2012**, *2012*, 2481–2486. [[CrossRef](#)]
16. Chui, S.S.-Y.; Lo, S.M.-F.; Charmant, J.P.H.; Orpen, A.G.; Williams, I.D. A Chemically Functionalizable Nanoporous Material $[\text{Cu}_3(\text{TMA})_2(\text{H}_2\text{O})_3]_n$. *Science* **1999**, *283*, 1148–1150. [[CrossRef](#)] [[PubMed](#)]
17. Ferey, G.; Serre, C.; Mellot-Draznieks, C.; Millange, F.; Surble, S.; Dutour, J.; Margiolaki, I. A Hybrid Solid with Giant Pores Prepared by a Combination of Targeted Chemistry, Simulation, and Powder Diffraction. *Angew. Chem. Int. Ed.* **2004**, *43*, 6296–6301. [[CrossRef](#)] [[PubMed](#)]
18. Horcajada, P.; Surble, S.; Serre, C.; Hong, D.-Y.; Seo, Y.-K.; Chang, J.-S.; Greneche, J.-M.; Margiolaki, I.; Ferey, G. Synthesis and catalytic properties of MIL-100(Fe), an iron(III) carboxylate with large pores. *Chem. Commun.* **2007**, 2820–2822. [[CrossRef](#)] [[PubMed](#)]
19. McCormick, L.J.; Morris, S.A.; Slawin, A.M.Z.; Teat, S.J.; Morris, R.E. Coordination Polymers of 5-Alkoxy Isophthalic Acids. *Cryst. Growth Des.* **2016**, *16*, 5771–5780. [[CrossRef](#)]
20. Yang, H.-B.; Northrop, B.H.; Zheng, Y.-R.; Ghosh, K.; Stang, P.J. Facile Self-Assembly of Neutral Dendritic Metalloclusters via Oxygen-to-Platinum Coordination. *J. Org. Chem.* **2009**, *74*, 7067–7074. [[CrossRef](#)] [[PubMed](#)]
21. Yang, J.-X.; Zhang, X.; Cheng, J.-K.; Yao, Y.-G. A novel 1D→2D interdigitated framework directed by hydrogen bonds. *J. Mol. Struct.* **2011**, *991*, 31–34. [[CrossRef](#)]
22. Gole, B.; Bar, A.K.; Mukherjee, P.S. Modification of Extended Open Frameworks with Fluorescent Tags for Sensing Explosives: Competition between Size Selectivity and Electron Deficiency. *Chem. Eur. J.* **2014**, *20*, 2276–2291. [[CrossRef](#)] [[PubMed](#)]
23. Zhang, D.-W.; Zhao, G.-Y. Synthesis, Crystal Structure, and Photoluminescent Property of a New 1D→2D Interdigitated Framework. *Synth. React. Inorg. Met. Org. Nano-Met. Chem.* **2015**, *45*, 524–526. [[CrossRef](#)]
24. Su, Y.; Li, X.; Li, X.; Pan, H.; Wang, R. Effects of hydroxy substituents on Cu(II) coordination polymers based on 5-hydroxyisophthalate derivatives and 1,4-bis(2-methylimidazol-1-yl)benzene. *CrystEngComm* **2015**, *17*, 4883–4894. [[CrossRef](#)]
25. Gole, B.; Bar, A.K.; Mukherjee, P.S. Multicomponent Assembly of Fluorescent-Tag Functionalized Ligands in Metal–Organic Frameworks for Sensing Explosives. *Chem. Eur. J.* **2014**, *20*, 13321–13336. [[CrossRef](#)] [[PubMed](#)]
26. Li, X.; Li, J.; Li, M.-K.; Fei, Z. Synthesis, structures and photocatalytic properties of two new Co(II) coordination polymers based on 5-(benzyloxy)isophthalate ligand. *J. Mol. Struct.* **2014**, *1059*, 294–298. [[CrossRef](#)]
27. Zhang, X.; Yang, J.-X.; Yao, Y.-G. Tail of the Organic Ligand Templated Metal-Organic Framework. *J. Inorg. Organomet. Polym. Mater.* **2012**, *22*, 1189–1193. [[CrossRef](#)]
28. Perry, J.J.; McManus, G.J.; Zaworotko, M.J. Sextuplet phenyl embrace in a metal–organic Kagomé lattice. *Chem. Commun.* **2004**, 2534–2535. [[CrossRef](#)] [[PubMed](#)]
29. Dance, I.; Scudder, M. The Sextuple Phenyl Embrace, a Ubiquitous Concerted Supramolecular Motif. *J. Chem. Soc. Chem. Commun.* **1995**, 1039–1040. [[CrossRef](#)]
30. Dance, I.; Scudder, M. Supramolecular Motifs: Concerted Multiple Phenyl Embraces between Ph₄P⁺ Cations Are Attractive and Ubiquitous. *Chem. Eur. J.* **1996**, *2*, 481–486. [[CrossRef](#)] [[PubMed](#)]
31. Sun, X.-F.; You, J.-M.; Xu, X.-H.; Li, X.-J. A Zn(II) Metal-organic Framework Consisting of Hexagonal Cavities Constructed by Benzyl-functionalized 5-Aminoisophthalate. *Chin. J. Struct. Chem.* **2015**, *34*, 562–568. [[CrossRef](#)]
32. Gupta, M.; Ahmad, M.; Singh, R.; Mishra, R.; Sahu, J.; Gupta, A.K. Zn(II)/Cd(II) based coordination polymers synthesized from a semi-flexible dicarboxylate ligand and their emission studies. *Polyhedron* **2015**, *101*, 86–92. [[CrossRef](#)]
33. Chucholowski, A.; Fingerle, J.; Iberg, N.; Marki, H.P.; Muller, R.; Pech, M.; Rouge, M.; Schmid, G.; Tschopp, T.; Wessel, H.P. Sulfuric Acid Esters of Sugar Alcohols. U.S. Patent US5,521,160, 28 May 1996.
34. Gibson, H.W.; Wang, H.; Niu, Z.; Slebodnick, C.; Zhakharov, L.N.; Rheingold, A.L. Rotaxanes from Tetraclams. *Macromolecules* **2012**, *45*, 1270–1280. [[CrossRef](#)]
35. Kissel, L.; Pratt, R.H. XDISP Program in WinGX. *Acta Crystallogr.* **1990**, *A46*, 170–175. [[CrossRef](#)]
36. Farrugia, L.J. WinGX and ORTEP for Windows: An update. *J. Appl. Crystallogr.* **2012**, *45*, 849–854. [[CrossRef](#)]
37. Krause, L.; Herbst-Irmer, R.; Sheldrick, G.M.; Stalke, D. Comparison of silver and molybdenum microfocus X-ray sources for single-crystal structure determination. *J. Appl. Crystallogr.* **2015**, *48*, 3–10. [[CrossRef](#)] [[PubMed](#)]

38. *CrystalClear-SM Expert*, version 2.1; Rigaku Americas: The Woodlands, TX, USA, 2015.
39. Sheldrick, G.M. *SHELXT*—Integrated space group and crystal-structure determination. *Acta Crystallogr.* **2015**, *A71*, 3–8. [[CrossRef](#)] [[PubMed](#)]
40. Sheldrick, G.M. A short history of *SHELX*. *Acta Crystallogr. Sect. A* **2008**, *64*, 112–122. [[CrossRef](#)] [[PubMed](#)]
41. Sheldrick, G.M. Crystal structure refinement with *SHELXL*. *Acta Crystallogr.* **2015**, *C71*, 3–8. [[CrossRef](#)]
42. Hübschle, C.B.; Sheldrick, G.M.; Dittrich, B. ShelXle: A Qt user interface for *SHELXL*. *J. Appl. Cryst.* **2011**, *44*, 1281–1284. [[CrossRef](#)] [[PubMed](#)]



© 2017 by the authors. Licensee MDPI, Basel, Switzerland. This article is an open access article distributed under the terms and conditions of the Creative Commons Attribution (CC BY) license (<http://creativecommons.org/licenses/by/4.0/>).